

Impaired posttranslational processing and trafficking of an endosomal Na⁺/H⁺ exchanger NHE6 mutant (Δ^{370} WST³⁷²) associated with X-linked intellectual disability and autism



Alina Ilie^a, Erica Weinstein^a, Annie Boucher^a, R. Anne McKinney^b, John Orłowski^{a,*}

^a Department of Physiology, McGill University, Montreal, Canada

^b Department of Pharmacology and Therapeutics, McGill University, Montreal, Canada

ARTICLE INFO

Article history:

Available online 30 September 2013

Keywords:

NHE6
Recycling endosomes
Vesicular trafficking
Neurodegeneration
Intellectual disability

ABSTRACT

Na⁺/H⁺ exchanger NHE6/SLC9A6 is an X-linked gene that is widely expressed and especially abundant in brain, heart and skeletal muscle where it is implicated in endosomal pH homeostasis and trafficking as well as maintenance of cell polarity. Recent genetic studies have identified several mutations in the coding region of NHE6 that are linked with severe intellectual disability, autistic behavior, ataxia and other abnormalities. One such defect consists of an in-frame deletion of three amino acids (³⁷⁰Trp–Ser–Thr³⁷², Δ WST) that adjoin the predicted ninth transmembrane helix of the exchanger. To better understand the nature of this mutation, a NHE6 Δ WST construct was generated and assessed for its effects on the biochemical and cellular properties of the transporter. In transfected fibroblastic CHO and neuroblastoma SH-SY5Y cells, immunoblot analyses showed that the mutant protein was effectively synthesized, but its subsequent oligosaccharide maturation and overall half-life were dramatically reduced compared to wild-type. These changes correlated with significant accumulation of Δ WST in the endoplasmic reticulum, with only minor sorting to the plasma membrane and negligible trafficking to recycling endosomes. The diminished accumulation in recycling endosomes was associated with a significant decrease in the rate of endocytosis of cell surface Δ WST compared to wild-type. Furthermore, while ectopic expression of wild-type NHE6 enhanced the uptake of other vesicular cargo such as transferrin along the clathrin-mediated recycling endosomal pathway, this ability was lost in the Δ WST mutant. Similarly, in transfected primary mouse hippocampal neurons, wild-type NHE6 was localized in discrete puncta throughout the soma and neurites, whereas the Δ WST mutant displayed a diffuse reticular pattern. Remarkably, the extensive dendritic arborization observed in neurons expressing wild-type NHE6 was noticeably diminished in Δ WST-transfectants. These results suggest that deletion of ³⁷⁰Trp–Ser–Thr³⁷² leads to endoplasmic reticulum retention and loss of NHE6 function which potentially impacts the trafficking of other membrane-bound cargo and cell polarity.

© 2013 Elsevier Ltd. All rights reserved.

1. Introduction

Intellectual disability (ID) encompasses a broad spectrum of disorders characterized by marked deficits in cognitive ability (e.g., learning, reasoning, perception) and adaptive skills (e.g., communication, social interaction, self-care) and is estimated to afflict 1–3% of the human population (Leonard and Wen, 2002). The causes are also quite varied, ranging from environmental factors such as fetal exposure to noxious substances (e.g., alcohol, narcotics), malnutrition and infectious agents to chromosomal abnormalities (e.g., trisomy 21 or Down syndrome) and single-gene

mutations (e.g., *Fmr1*, fragile X syndrome), with genetic factors accounting for approximately half of the cases. Thus far, mutations in over 500 genes have been identified that result in ID, with a significant fraction (i.e., 102 genes) located on the X-chromosome (X-linked intellectual disability, XLID) (Inlow and Restifo, 2004; Vailend et al., 2008; Géczy et al., 2009; Ropers, 2010; Lubs et al., 2012). These genes are involved in diverse molecular and cellular processes, including DNA repair and recombination, chromatin remodeling, gene transcription, protein translation and modification, protein degradation, membrane excitability, signal transduction cascades, vesicular trafficking and fusion, synapse formation and maturation, mitochondrial function, regulation of actin cytoskeletal dynamics, cell adhesion, cell cycle progression and apoptosis. Given this heterogeneity, it is not surprising to find that disruption of their activities can impact neural development and

* Corresponding author. Address: Department of Physiology, McGill University, McIntyre Medical Sciences Bldg., 3655 Promenade Sir-William-Osler, Montreal, Quebec H3G 0B1, Canada. Tel.: +1 514 398 8335.

E-mail address: john.orlowski@mcgill.ca (J. Orłowski).

function at many different levels, ranging from the macro-organization of the central nervous system (CNS) and formation of neuronal networks to the micro-architecture and plasticity of synapses implicated in learning and memory (Vaillend et al., 2008; Humeau et al., 2009).

A recent inclusion to the list of genes implicated in XLID is *SLC9A6* (Gilfillan et al., 2008) which is located at chromosomal position Xq26.3 and encodes a pH-regulating transporter, the alkali cation (Na^+ or K^+)/ H^+ exchanger NHE6 isoform. NHE6 is widely expressed in humans, but is most abundant in excitable tissues such as the brain, heart and skeletal muscle (Orlowski and Grinstein, 2007). Within non-neuronal cells, NHE6 localizes predominantly to transferrin receptor-containing recycling endosomes and to a lesser extent at the plasma membrane (Miyazaki et al., 2001; Brett et al., 2002) where it has been implicated in regulating intravesicular pH and cargo trafficking (Ohgaki et al., 2010; Xinhan et al., 2011) as well as maintenance of epithelial apical cell polarity (Ohgaki et al., 2010). In mouse brain, *in situ* analysis (www.brain-map.org) detected *Nhe6* transcripts throughout the CNS (Lein et al., 2004). More detailed immunocytochemical examination of hippocampal CA1 pyramidal neurons revealed the presence of NHE6 throughout the soma and dendrites in vesicles that are enriched at dendritic spines, the postsynaptic compartment, but also at excitatory presynaptic terminals (Deane et al., 2013). Within dendrites and spines, NHE6 partially colocalized with known markers of early (*i.e.*, EEA1) and recycling endosomes (*i.e.*, transferrin, syntaxin-13), but also with vesicles containing the glutamatergic AMPA (α -amino-3-hydroxy-5-methyl-4-isoxazolepropionic acid) receptor subunit GluA1. AMPA receptors are responsible for the majority of fast excitatory synaptic transmission in the brain. Importantly, recycling endosomes transport GluA1-containing AMPA receptors and lipids into and out of synapses in an activity-dependent manner that is thought to modulate the morphology of dendritic spines and certain forms of synaptic plasticity such as long-term potentiation and depression, cellular mechanisms postulated to underlie learning and memory (Yuste and Bonhoeffer, 2001; Shi et al., 2001; Park et al., 2004, 2006). In this regard, NHE6-containing endosomes are also recruited to dendritic spines following NMDA receptor-dependent long-term potentiation, implicating a potential role for NHE6 in synaptic plasticity (Deane et al., 2013).

In humans, several mutations (*i.e.*, frameshift, nonsense and deletions) in NHE6 have been identified (Gilfillan et al., 2008; Schroer et al., 2010; Tzsachach et al., 2011; Takahashi et al., 2011; Riess et al., 2013; Mignot et al., 2013) that are associated with severe intellectual disability, microcephaly (accompanied in some cases by cerebellar atrophy), epilepsy, ataxia, lack of speech and in some cases frequent laughter/smiling; a phenotype that closely mimics Angelman syndrome and termed Christianson syndrome based on earlier XLID chromosomal mapping studies (Christianson et al., 1999). The majority of these mutations result in the introduction of a premature stop codon in the ion translocation domain of the exchanger and hence most likely cause complete loss of function. Conversely, one of these mutations that resulted in an in-frame deletion of two highly conserved amino acids ($^{255}\text{Glu-Ser}^{256}$) in the predicted seventh transmembrane helix was translated to completion but was found to be highly unstable and rapidly degraded (Roxrud et al., 2009). Genetic ablation of NHE6 in mice also causes a neurodegenerative phenotype, though the effect is less pronounced and characterized by motor hyperactivity and cerebellar dysfunction (Stromme et al., 2011).

In addition to the above, Garbern and colleagues (Garbern et al., 2010) recently identified another in-frame deletion mutation in human NHE6 that excises three amino acids, $^{370}\text{Trp-Ser-Thr}^{372}$ (NHE6 Δ WST), that border the predicted ninth transmembrane helix and are relatively conserved in organellar-type NHEs (*i.e.*, NHE6,

7 and 9) but not in plasma membrane-type NHEs (*i.e.*, NHE1–5). This mutation elicits a subset of the symptoms present in Christianson syndrome (*i.e.*, mental retardation, mutism, epilepsy), but is distinguished by the additional manifestation of autistic behavior, late-onset progressive ataxia, wide-spread neuronal loss and neuronal and glial inclusions of the microtubule-binding protein tau in cortical and sub-cortical regions. The latter is more characteristic of adult-onset neurodegenerative disorders, collectively known as tauopathies, which include Alzheimer's disease, Pick's disease and others (Morris et al., 2011).

In order to gain a better understanding of the nature of this defect, we examined some of the biochemical and cellular properties of NHE6 Δ WST. The results show that NHE6 Δ WST is largely confined to the endoplasmic reticulum, though a minor fraction is delivered to the cell surface but is not subsequently sorted to recycling endosomes. Concomitantly, unlike the wild-type transporter, NHE6 Δ WST lacked the ability to regulate the trafficking of endosomal cargo. When examined in transfected primary mouse hippocampal neurons, NHE6 Δ WST also showed a reticular pattern of expression and remarkably, the extensive dendritic arborization observed in cells expressing wild-type NHE6 was noticeably diminished in Δ WST-transfectants. These results suggest that in-frame deletion of $^{370}\text{Trp-Ser-Thr}^{372}$ leads to endoplasmic reticulum retention and loss of NHE6 function which potentially impacts the trafficking of other membrane-bound cargo and maintenance of cell polarity.

2. Materials and methods

2.1. Reagents

Mouse monoclonal anti-hemagglutinin (HA) antibody was purchased from Covance Inc. (Berkeley, CA); monoclonal anti-glyceraldehyde-3-phosphate dehydrogenase (GAPDH) antibody was obtained from Abcam Inc. (Cambridge, MA); mouse monoclonal anti-Flag M2 antibody was from Sigma; rabbit polyclonal anti-calnexin antibody was from Enzo Life Sciences (Farmingdale, NY). Horseradish peroxidase-conjugated secondary IgG antibodies were purchased from Jackson ImmunoResearch Laboratories (West Grove, PA). All Alexa Fluor[®] conjugated secondary antibodies and probes were purchased from Molecular Probes (Eugene, OR).

Alpha-minimum essential medium (α -MEM), fetal bovine serum, penicillin/streptomycin and trypsin-EDTA were purchased from Wisent (Saint-Bruno, QC, Canada). The DMEM/F12 medium was from Corning. All other chemical and reagents were obtained from BioShop Canada (Burlington, ON, Canada), Sigma or Fisher Scientific and were of the highest grade available.

2.2. Recombinant DNA constructs and mutagenesis

The long transcript splice-variant of human NHE6 (NHE6v1; NCBI refseq NM_001042537) was cloned from a human brain Matchmaker[™] cDNA library (Clontech) using PCR methodology and was engineered to contain the influenza virus hemagglutinin (HA) (YPYDVPDYAS) epitope at its extreme C-terminal end. This construct was termed wild-type NHE6_{HA} (NHE6wt_{HA}) and inserted into the *HindIII* and *XbaI* sites of the mammalian expression vector pcDNA3 (Invitrogen). NHE6wt_{HA} was then used as a template to engineer the in-frame triple deletion mutation $^{370}\text{Trp-Ser-Thr}^{372}$ (NHE6 Δ WST_{HA}) by PCR mutagenesis. The same template (NHE6wt_{HA}) was also used to introduce a triple Flag epitope (3x DYKDDDDK) in the first extracellular loop, generating a construct termed $_{3F}$ NHE6wt_{HA}. This construct was further modified to contain the Δ WST mutation. GFP- and mCherry (ChFP) C-terminal-tagged forms of NHE6 wild-type and Δ WST mutant were

constructed by insertion between the *XhoI* and *HindIII* restriction sites of the pAcGFP1-N1 vector (BD Biosciences Clontech, Palo Alto, CA). Insertion of the different epitope tags in the various positions did not alter the biochemical properties or cellular distribution of exogenous NHE6 compared to the endogenous protein (Brett et al., 2002) (unpublished observations, A. Ilie and J. Orłowski). All constructs were sequenced to insure that no additional mutations were introduced during PCR.

2.3. Cell culture

AP-1 (Chinese hamster ovary cells devoid of plasma membrane Na^+/H^+ exchange NHE1 activity) (Rotin and Grinstein, 1989) and HeLa cells were maintained in α -MEM supplemented with 10% fetal bovine serum, penicillin (100 units/mL), streptomycin (100 $\mu\text{g}/\text{mL}$) and 25 mM NaHCO_3 (pH 7.4). Human neuroblastoma SH-SY5Y cells were cultured in high glucose Dulbecco's Modified Eagle Medium (DMEM)/Ham's F12 medium supplemented with 10% fetal bovine serum. Primary cultures of mouse hippocampal neurons were generated postnatal day 0–2 as previously described (Deane et al., 2013). Briefly, enzymatically dissociated neurons and glial cells were suspended in DMEM supplemented with 1% penicillin–streptomycin, 10% fetal bovine serum and 0.6% glucose. Cells were then plated onto poly-D-lysine-coated 10-mm coverslips at a density of 12,000 cells/ cm^2 and placed in an incubator at 37 °C. After 24 h, plating media was replaced with neuronal growth media consisting of Neurobasal-A[®], 2% B-27[®] supplement, 1% GlutaMAXTM and 1% penicillin–streptomycin. Neurons were fed every 3–4 days, maintained 10–12 days *in vitro* prior to subsequent experimentation. All cells were incubated in a humidified atmosphere of 95% air, 5% CO_2 at 37 °C.

To generate AP-1 cells stably expressing $3\text{F-NHE6}_{\text{HA}}$ wild-type or ΔWST , cells were grown to subconfluence in 6-well plates and transfected with plasmid DNA (1 $\mu\text{g}/\text{well}$) using Lipofectamine[™] reagent according to the manufacturer's instructions. Twenty-four hours after transfection, cells were split (1:50) into 10-cm dishes and selected for stably expressing clones in α -MEM culture medium supplemented with G418 sulfate (800 $\mu\text{g}/\text{mL}$) over a 3-weeks period.

2.4. Western blotting

For western blot analysis, AP-1 or SH-SY5Y cells were grown in 10-cm dishes and transiently transfected with 5 μg of plasmid DNA encoding NHE6_{HA} wild-type or mutant constructs using Lipofectamine2000[™] (Invitrogen) according to the manufacturer's recommended procedure. Forty-eight hours post-transfection, cell lysates were obtained by washing cells twice on ice with ice-cold PBS, followed by scraping in 0.5 mL of lysis buffer (0.5% NP40/0.25% sodium deoxycholate/PBS supplemented with a tablet of protease inhibitor cocktail (Roche Diagnostics)). Lysates were incubated for 30 min on a rocker at 4 °C, and then centrifuged for 20 min at 4 °C to pellet the nuclei and cellular debris. 10–20 μg of protein from the resulting supernatants were eluted in sodium dodecyl sulfate (SDS)-sample buffer (50 mM Tris-HCl, pH 6.8, 1% SDS, 50 mM dithiothreitol, 10% glycerol, 1% bromophenol blue) and subjected to 9% SDS-polyacrylamide gel electrophoresis (SDS-PAGE), then transferred to polyvinylidene fluoride (PVDF) membranes (Millipore, Nepean, Ontario, Canada) for immunoblotting. The membranes were blocked with 5% non-fat skim milk for 1 h, then incubated with the specified primary antibodies (mouse monoclonal HA 1:5000 or mouse monoclonal GAPDH 1:50,000) in PBS containing 0.1% Tween 20, followed by extensive washes and incubation with goat anti-mouse horseradish peroxidase (HRP)-conjugated secondary antibody for 1 h. Immunoreactive

bands were detected using Western Lightning[™] Plus-ECL blotting detection reagents (Perkin Elmer Inc., Waltham, MA).

2.5. Cell surface biotinylation

AP-1 cells stably expressing $3\text{F-NHE6}_{\text{HA}}$ wild-type or mutant constructs were cultured in 10-cm dishes to sub-confluence, placed on ice and washed three times with ice-cold PBS containing 1 mM MgCl_2 and 0.1 mM CaCl_2 , pH 8.0 (PBS-CM). Next, cells were incubated at 4 °C for 30 min with the membrane-impermeable reagent N-hydroxysulfosuccinimide-SS-biotin (0.5 mg/mL) (ThermoScientific, Rockford, IL). Cells were washed and incubated twice in quenching buffer (50 mM glycine in PBS-CM) for 7 min each on ice to remove unreacted biotin. After two more washes in PBS-CM, the cells were lysed for 30 min on ice, and then centrifuged at 16,000g for 20 min at 4 °C to remove insoluble cellular debris. A fraction of the resulting supernatant was removed and this represents the total fraction. The remaining supernatant was incubated with 100 μL of 50% NeutrAvidin[®] Agarose Resin slurry (Fisher Scientific, Whitby, ON, Canada) in lysis buffer overnight at 4 °C to extract biotinylated membrane proteins. The proteins were then resolved by SDS-PAGE and analyzed by western blotting.

2.6. Stability of NHE6 wild-type and ΔWST mutant

To determine the stability of wild-type and mutant NHE6, AP-1 cells stably expressing $3\text{F-NHE6}_{\text{HA}}$ wild-type or mutant constructs were grown to confluence in 6-well plates. To inhibit new protein synthesis, cells were treated with cycloheximide (150 $\mu\text{g}/\text{mL}$) in α -MEM supplemented with 10% FBS and penicillin/streptomycin for up to 24 h. At specific time points, cells were lysed, protein concentrations were measured, and equal quantities of protein were subjected to SDS-PAGE and immunoblotting with mouse monoclonal anti-HA and anti-GAPDH antibodies. The intensity of the bands was quantified by densitometry of X-ray films exposed in the linear range and analyzed using ImageJ.

2.7. Fluorescence-based endocytosis assay

AP-1 cells were transiently transfected with 6 μg of $3\text{F-NHE6}_{\text{HA}}$ wild-type or mutant cDNA constructs. Twenty-four hours post-transfection, cells were transferred to 12 well-plates and grown for an additional 24 h. Cells were chilled on ice, washed with ice-cold PBS supplemented with 0.1 mM CaCl_2 and 1 mM MgCl_2 (PBS-CM, pH 7.4), blocked in 10% goat serum/PBS-CM and then incubated with a mouse monoclonal anti-Flag antibody (1:3000) (Sigma) on ice. Internalization of the bound antibody was initiated by incubating the cells with warm (37 °C) α -MEM for the indicated time points and terminated by placing the plates on ice. Cells were washed and labeled with goat anti-mouse HRP-conjugated secondary antibody (1:1000) (GE Healthcare). After extensive washes with PBS-CM, cells were treated on ice with Amplex[®] Red reagent (Invitrogen). Aliquots were transferred to 96-well plates and fluorescence readings were taken with a POLARstar OPTIMA (BMG Labtech, Inc., Offenburg, Germany) plate reader using 544-nm excitation and 590-nm emission wavelengths. All experiments were performed in triplicates and repeated at least 3 times. Results were expressed as a percentage of the fluorescence recorded prior to internalization, after subtraction of the value measured with mock-transfected cells. Results are shown as mean \pm standard error of the mean (S.E.M.).

2.8. Immunofluorescence confocal microscopy

To examine the subcellular localization of NHE6, AP-1 or SH-SY5Y cells were grown in 35-mm dishes and transfected with

NHE6_{HA} wild-type or Δ WST mutant. Twenty-four hours post-transfection, the cells were transferred to 1.5 μ g/mL fibronectin-coated glass coverslips and further cultured for 24 h. Cells were loaded with transferrin-Alexa594 (Tfn-Alexa⁵⁹⁴; 10 μ g/mL) for 45 min, and then fixed in 4% paraformaldehyde/PBS for 20 min at room temperature, permeabilized in 0.1% saponin in PBS for 20 min, followed by blocking in 10% goat serum, 0.01% saponin, 0.1 M glycine, in PBS for 1 h. Subsequently, the cells were incubated with mouse monoclonal anti-HA (1:1000) antibody for 2 h at room temperature. Next, cells were washed 4 times with blocking solution, and then incubated with anti-mouse Alexa Fluor[®] 488-conjugated secondary antibody (1:2000) for 1 h at room temperature. After extensive washes with PBS, cover slips were mounted onto glass slides with Aqua Poly/Mount mounting medium (Polysciences Inc., Warrington, PA).

For colocalization studies, AP-1 cells expressing NHE6_{HA} wild-type or Δ WST mutant were co-labeled with mouse monoclonal anti-HA (1:1000) and rabbit polyclonal anti-calnexin antibodies for 2 h at room temperature, followed by goat anti-mouse Alexa⁴⁸⁸- and goat anti-rabbit Alexa⁵⁶⁸-conjugated secondary antibodies.

To examine surface expression, AP-1 cells expressing 3F-NHE6_{HA} wild-type or Δ WST were incubated with Tfn-Alexa⁵⁹⁴, fixed, left unpermeabilized and then incubated with monoclonal anti-Flag antibody (1:1500), followed by Alexa-488-conjugated secondary antibody to label the surface pool of NHE6.

Mouse primary hippocampal neurons (10–12 days *in vitro*) were transfected with NHE6_{ChFP} wild-type or Δ WST mutant using calcium phosphate-DNA coprecipitation (Jiang and Chen, 2006), fixed in 4% paraformaldehyde/PBS for 20 min at room temperature and mounted onto glass coverslips. Cells were examined by laser scanning confocal microscopy on a Zeiss LSM 710 Meta, with images acquired using a 63x/1.4 N.A. oil immersion objective lens. Channels were acquired sequentially to prevent spectral overlap of fluorophores. Optical sections of 250–500 nm were taken; frame averaged 3x at low resolution or line-averaged 2x at high resolution, to improve the signal-to-noise ratio. Images were analyzed using ZEN software and Corel[®] CorelDraw[™] X5.

2.9. Flow cytometry

To measure transferrin uptake by flow cytometry, HeLa cells were transfected with GFP alone, NHE6_{GFP} wild-type or Δ WST mutant, using FuGene6 (Promega). Forty-eight hour after transfection, the cells were serum-depleted for 2 h and then incubated with Alexa Fluor[®] 633-conjugated transferrin (Tfn-Alexa⁶³³, 10 μ g/mL) for 5 min at 37 °C, in the absence or presence of 10-fold excess unlabelled transferrin, followed by washes to remove unbound transferrin. Cells were detached from the plates by trypsinization and 5 μ L of the cell viability dye 7-amino-actinomycin D (7-AAD, eBioscience) was added to each cell suspension. Cells were analyzed by flow cytometry using a FACS Aria Sorter (Becton Dickinson, San Jose, CA). A gate was set around the GFP-positive cells and the amount of Tfn-Alexa⁶³³ taken up by 10⁴ GFP-expressing live cells (*i.e.*, 7-AAD negative) was measured using the BD FACS Diva software. Data were normalized and represent mean \pm S.E.M. of three different experiments. Statistical significance was established using a paired two-tailed Student's *t*-test.

3. Results

3.1. Biosynthetic maturation of NHE6 Δ WST is impaired

The human NHE6 gene transcript is subject to alternate splicing resulting in three mRNA variants (NHE6v1, v2 and v3) that differ at their 5' end. Splice-variant NHE6v1 (NCBI NM_001042537)

encodes the longest transcript (701 amino acids); splice-variant NHE6v2 (NCBI NM_006359) uses an alternate in-frame splice site in the 5' coding region, resulting in a shorter protein that lacks 32 amino acids (amino acids 145–176) located in the predicted second extracellular loop of NHE6v1; and splice-variant NHE6v3 (NCBI NM_001177651) lacks a portion of the 5' coding region and initiates translation at a downstream start codon (Met⁵³ of NHE6v1). To examine the impact of deletion of ³⁷⁰Trp-Ser-Thr³⁷² on NHE6 function, the Δ WST mutation was engineered into an HA-epitope tagged form of the longest wild-type (wt) splice-variant NHE6v1 (simply called NHE6wt_{HA}). The NHE6v1 version was initially chosen for study as it appeared to be more efficiently processed to the mature fully-glycosylated form relative to its immature core-glycosylated form compared to the NHE6v2 variant in transfected cells (unpublished data). The molecular basis for this is unclear, but may reflect the fact that the v1 variant contains two glycosylation sites in its second extracellular loop whereas the v2 contains only one (unpublished data) which may improve

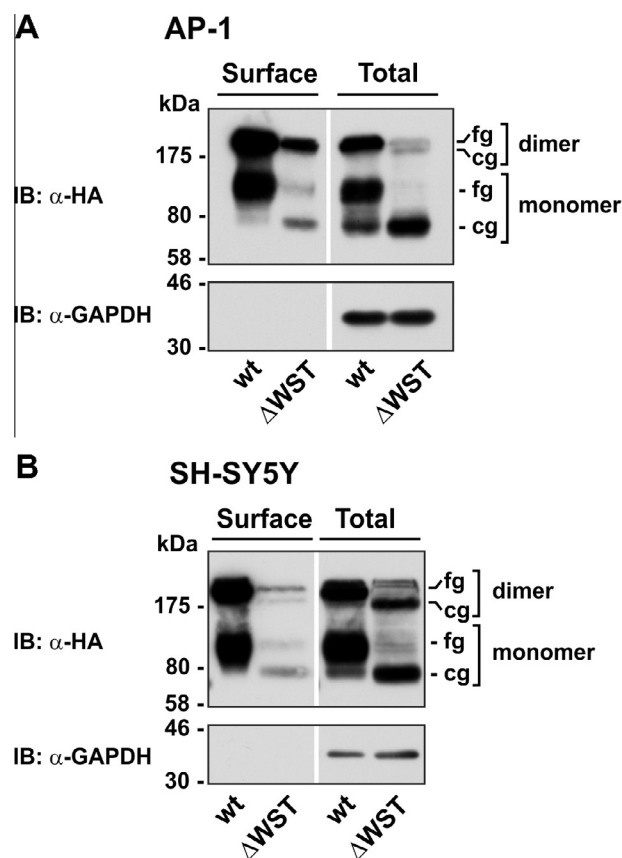


Fig. 1. Expression of NHE6 wild-type and Δ WST mutant proteins in transfected AP-1 and SH-SY5Y cells. (A) AP-1 and (B) SH-SY5Y cells were transfected with NHE6_{HA} wild-type or the Δ WST mutant. Plasma membrane proteins were labeled with biotin as described in materials and methods. Total cell lysates were prepared and a portion representing the total fraction was removed. The remaining supernatant was incubated with NeutrAvidin[®] Agarose beads to extract the biotinylated cell surface proteins. For total cell lysates, aliquots representing ~1.75% (20 μ g protein) of the original lysates of NHE6wt_{HA} and NHE6 Δ WST_{HA}-transfectants were examined by SDS-PAGE. For the cell surface fractions, 50% and 100% of the entire biotinylated proteins extracted from total lysates of NHE6wt_{HA} and NHE6 Δ WST_{HA}-transfectants, respectively, were examined by SDS-PAGE. The immunoblots were probed with a mouse monoclonal anti-HA antibody to detect NHE6 (upper panels) and a monoclonal anti-GAPDH antibody (lower panels). NHE6 migrates as multiple bands: (1) a slower migrating, high molecular weight band (~200 kDa) representing the dimeric form of the exchanger that does not fully dissociate under SDS-PAGE conditions; (2) a mature, fully-glycosylated (fg) form of the monomeric protein (~100 kDa); and (3) a faster migrating, lower molecular weight band (~77 kDa) characteristic of the immature core-glycosylated (cg) monomer. The data are representative of three independent experiments.

protein folding and processing as has been proposed for some glycosylated proteins (Dorner et al., 1987; Ruddock and Molinari, 2006; Mitra et al., 2006). Chinese hamster ovary AP-1 cells or human neuroblastoma SH-SY5Y cells were transiently transfected with NHE6wt_{HA} or NHE6ΔWST_{HA} and the expression of these constructs was evaluated by immunoblotting with an anti-HA antibody 48 h following transfection. These cell lines were selected for study because the level of endogenous NHE6 is negligible in AP-1 cells (below detection sensitivity) whereas it is well expressed in SH-SY5Y cells (Deane et al., 2013). Since NHEs assemble as homodimers, this would allow us to examine the impact of the mutation on the processing and distribution of a homozygous (ΔWST/ΔWST) or potentially heterozygous (+/ΔWST) dimer. As presented in Fig. 1A and B (upper panels) and consistent with earlier findings (Miyazaki et al., 2001), analyses of total cell lysates from AP-1 and SH-SY5Y cells showed that NHE6wt_{HA} migrated identically in both preparations as multiple bands: (1) a slower migrating, high molecular weight band (~200 kDa) representing the dimeric form of the exchanger that does not fully dissociate under SDS-PAGE conditions; (2) a mature, fully-glycosylated form of the monomeric protein (~100 kDa); and (3) a faster migrating, lower molecular weight band (~77 kDa) characteristic of the immature core-glycosylated monomer. By contrast, the NHE6ΔWST_{HA} mutant from both cell lines migrated predominantly as a single band at the level of the core-glycosylated monomer. However, fainter bands corresponding to the fully-glycosylated monomer and the core- and fully-glycosylated dimers were visible, suggesting that a minor fraction of the mutant protein is capable of undergoing further processing and oligosaccharide maturation. Similar results were also obtained using the shorter NHE6v2 splice variant (data not shown), suggesting that the mutation broadly affects the NHE6 splice variants.

Although NHE6 accumulates in endosomes, a minor proportion (*i.e.*, ~5% of total NHE6) can be detected at the plasma membrane as the transporter transits along the biosynthetic and recycling endosomal pathways (Brett et al., 2002). To investigate whether some of the ΔWST mutant can traffic to the cell surface, plasmalemmal localization was measured biochemically in transfected AP-1 and SH-SY5Y cells using a cell surface biotinylation assay (Le Bivic

et al., 1989). As shown in Fig. 1A and B (upper panels), the mutant protein reached the cell surface of both cell lines mainly in its core-glycosylated form, although some of the fully-glycosylated protein as well as undissociated dimers were also detected. The surface abundance of the wild-type protein was significantly higher compared to the mutant, and essentially only the glycosylated forms were detected at the cell surface. Comparative densitometric analysis of the cell surface abundance of wild-type and ΔWST relative to the total protein present in the lysates showed that ~5% of the wild-type protein was present at the cell surface, whereas <1% of the mutant trafficked to the plasma membrane. To ensure that the extracted cell surface biotinylated proteins were not contaminated with intracellular proteins, the immunoblots were probed with an antibody that recognizes the glycolytic enzyme GAPDH. GAPDH was readily detected in total cell lysates but not in the plasmalemmal fractions, thereby confirming the veracity of the extraction protocol (Fig. 1A and B, lower panels). The essentially identical patterns of expression in both cell lines as assessed by immunoblotting of cell extracts also suggest that the presence of endogenous NHE6 in the SH-SY5Y cells also did not visibly alter the processing of the exogenous NHE6ΔWST_{HA} mutant.

To further confirm the presence of NHE6 at the cell surface using imaging techniques, a triple Flag epitope-tag was inserted in the first extracellular loop of wild-type and mutant NHE6_{HA} (3F-NHE6wt_{HA} and 3F-NHE6ΔWST_{HA}). Insertion of epitopes in the first extracellular loop has been shown to have no discernible effect on the processing, trafficking and function of the transporter (Brett et al., 2002) (A. Ilie and J. Orłowski, unpublished data). Using confocal microscopy, both the wild-type and mutant constructs were detected at the cell surface of transiently transfected AP-1 cells (Fig. 2). These results indicate that the peptide fragment ³⁷⁰Trp-Ser-Thr³⁷² is important, but not absolutely essential, for the biosynthetic maturation, post-translational modification and dimeric assembly of NHE6.

3.2. The NHE6ΔWST mutant is mislocalized in cells

The arrested posttranslational processing of the NHE6ΔWST_{HA} mutant as revealed by the immunoblotting analyses presented in

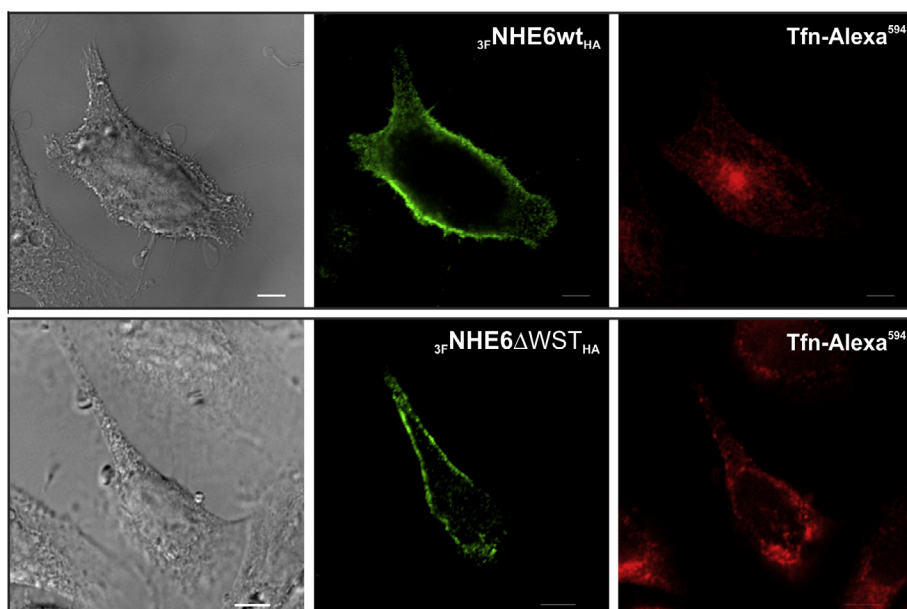


Fig. 2. Surface expression of NHE6 wild-type and ΔWST mutant in AP-1 cells. Transfected AP-1 cells expressing 3F-NHE6wt_{HA} or 3F-NHE6ΔWST_{HA} mutant were incubated with fluorescently-labeled transferrin (Tfn-Alexa⁵⁹⁴, 10 μg/mL) for 45 min, then fixed in 4% paraformaldehyde but left non-permeabilized (*i.e.*, not treated with detergent), followed by incubation with a primary anti-Flag antibody and an Alexa-488-conjugated secondary antibody to label the cell surface pool of NHE6. The cells were examined by confocal microscopy. Scale bars represent 5 μm.

Fig. 1 suggested that its intracellular distribution might be altered. To examine this possibility, AP-1 or SH-SY5Y cells transiently expressing NHE6^{wt}_{HA} or NHE6 Δ WST_{HA} were loaded with red fluorescently-labeled transferrin (Tfn–Alexa⁵⁹⁴) and imaged by confocal microscopy. As expected, NHE6^{wt}_{HA} was sorted to punctate vesicles that largely overlapped with Tfn–Alexa⁵⁹⁴ in both AP-1 and SH-SY5Y cells (Fig. 3A and B, respectively, upper panels). In contrast, the NHE6 Δ WST_{HA} mutant showed a diffuse reticular distribution that did not significantly overlap the Tfn–Alexa⁵⁹⁴-labeled compartments (Fig. 3A and B, lower panels), but instead was more reminiscent of the endoplasmic reticulum (ER). Further dual-immunolabelling with antibodies that recognized the ER marker calnexin confirmed that indeed the fluorescence pattern for NHE6 Δ WST_{HA} closely matched those for calnexin (Fig. 4B), whereas NHE6^{wt}_{HA} showed minimal colocalization (Fig. 4A).

3.3. The internalization rate of the NHE6 Δ WST mutant is diminished

Having established that a small fraction of ³F-NHE6 Δ WST_{HA} can accumulate at the cell surface, we next assessed whether its rate of internalization was different from that of the wild-type protein. To this end, ³F-NHE6^{wt}_{HA} and ³F-NHE6 Δ WST_{HA} were tran-

siently expressed in AP-1 cells and their internalization was examined using a fluorescence-based endocytosis protocol (Barriere et al., 2011). This assay measures the loss of cell surface immunoreactivity of epitope-tagged plasma membrane proteins by use of an enzyme-linked immunosorbent assay. Forty-eight hours after transfection, the cells were placed on ice and incubated with a mouse monoclonal anti-Flag antibody to label cell surface ³F-NHE6_{HA}, followed by internalization at 37 °C for various times ranging from 5 to 30 min. As shown in Fig. 5, wild-type NHE6 was rapidly endocytosed (~40% internalized after 5 min), whereas the Δ WST mutant displayed a much slower rate of internalization (~5% after 5 min).

3.4. The stability of the NHE6 Δ WST mutant is reduced

As shown above, the majority of the mutant protein was retained in the ER possibly due to impaired protein folding, suggesting that it might be subject to more rapid degradation than its wild-type counterpart. In order to examine the stability of the mutant protein, AP-1 cells stably expressing ³F-NHE6^{wt}_{HA} and ³F-NHE6 Δ WST_{HA} were treated with cycloheximide for 2, 4, 8, or 24 h in order to block *de novo* protein synthesis. Cell lysates were

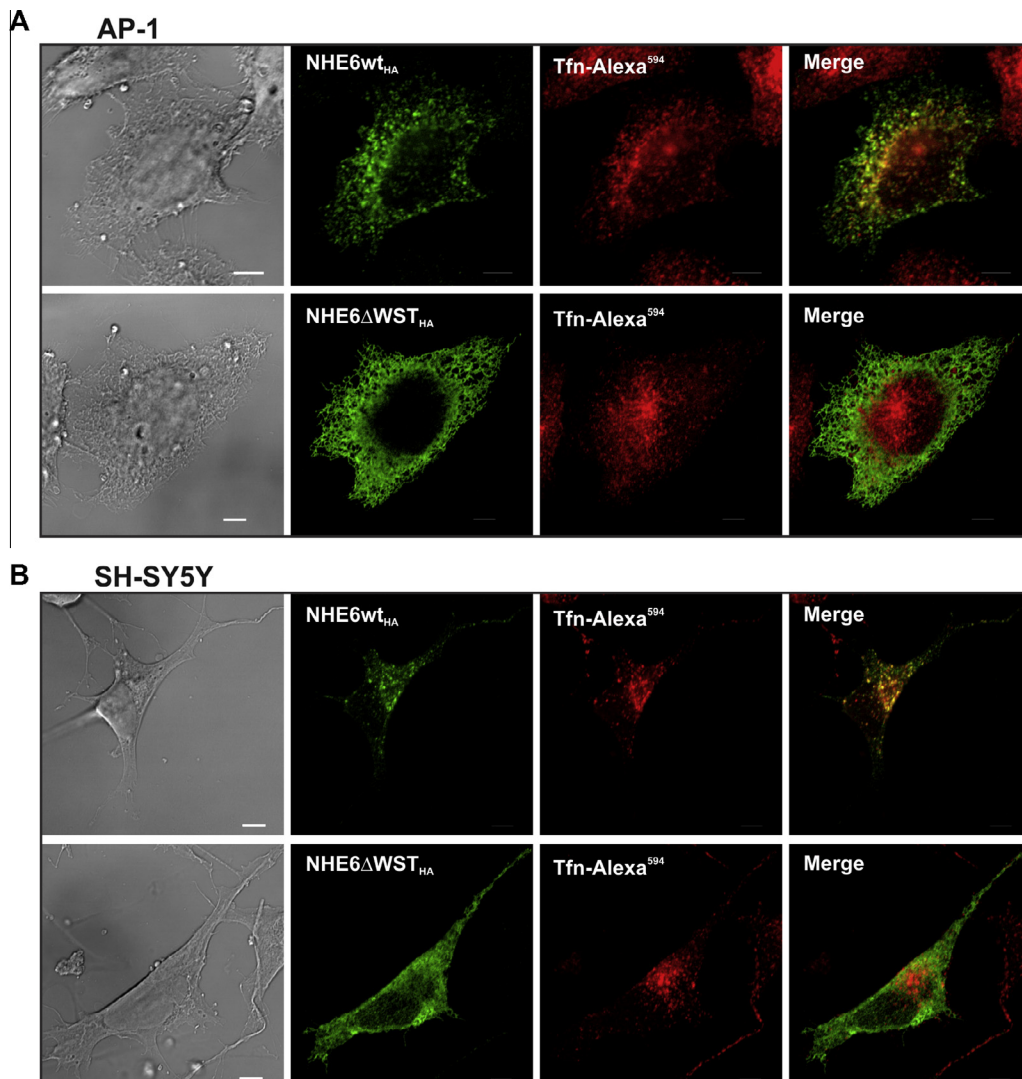


Fig. 3. Subcellular distribution of NHE6 wild-type and Δ WST mutant in AP-1 and SH-SY5Y cells. (A) AP-1 and (B) SH-SY5Y cells were grown on fibronectin-coated glass coverslips and transiently transfected with NHE6^{wt}_{HA} (upper panels) or NHE6 Δ WST_{HA} (lower panels). Forty-eight hours after transfection, cells were loaded with fluorescently-labeled transferrin (Tfn–Alexa⁵⁹⁴, 10 μ g/mL) for 45 min, fixed in 4% paraformaldehyde, permeabilized, mounted onto glass slides and then examined by confocal microscopy. Scale bars represent 5 μ m.

obtained at the indicated time points and proteins were visualized by SDS-PAGE and immunoblotting and the expression levels were quantitated by densitometry. As shown in Fig. 6, the $3F$ NHE6wt_{HA} protein and the loading control, GAPDH, were very stable even after 24 h of treatment with cycloheximide. In contrast, the deletion mutant was rapidly degraded with a half-life ($t_{1/2}$) of ~ 8 h.

3.5. NHE6wt-mediated stimulation of transferrin uptake in cells is lost in the Δ WST mutant

Previous studies (Xinhan et al., 2011) using biochemical assays and light microscopy have shown that manipulation of NHE6 expression in HeLa cells selectively regulates internalization of other vesicular cargo that are dependent on the endocytic adaptor protein

AP2 and clathrin, such as the ligand-activated transferrin receptor. To determine if NHE6 Δ WST can regulate internalization of transferrin similar to its wild-type counterpart, we used an analogous flow cytometry-based approach to measure uptake of fluorescently-labeled transferrin (Tfn-Alexa⁶³³). For these experiments, HeLa cells were also used instead of AP-1 or SH-SY5Y cells because the signal to noise ratio was much greater at the early, linear phase of endocytosis (i.e., 5 min uptake), presumably due to higher abundance of the transferrin receptor. To this end, internalization of Tfn-Alexa⁶³³ was monitored by flow cytometry in living HeLa cells expressing GFP or GFP-tagged constructs of NHE6wt or NHE6 Δ WST. This uptake was distinguished from non-specific internalization of Tfn-Alexa⁶³³ in non-viable cells by their ability to exclude the membrane-impermeant fluorescent dye 7-amino actinomycin D (7-AAD). The median

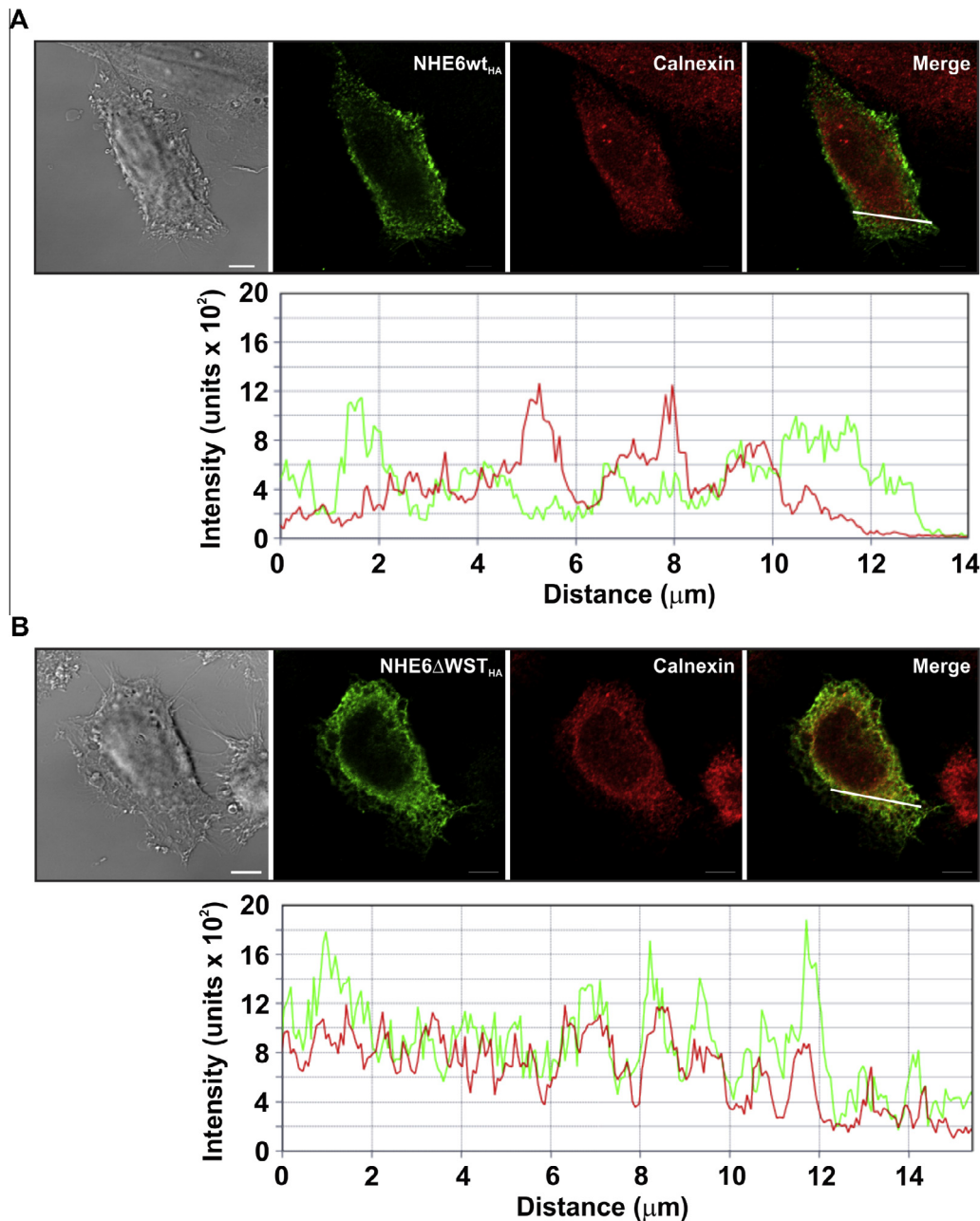


Fig. 4. Colocalization of NHE6 Δ WST with the ER resident protein calnexin in AP-1 cells. AP-1 cells transiently expressing (A) NHE6wt_{HA} or (B) NHE6 Δ WST_{HA} were co-immunolabelled for endogenous calnexin. Images are presented in the upper panels. Fluorescence intensity line scans of a selected region of the cells displayed in the upper panels (indicated by white lines) are represented in the lower panels. The data show a high degree of overlap of the mutant, but not wild-type, NHE6 with the ER marker calnexin. Scale bars represent 5 μm .

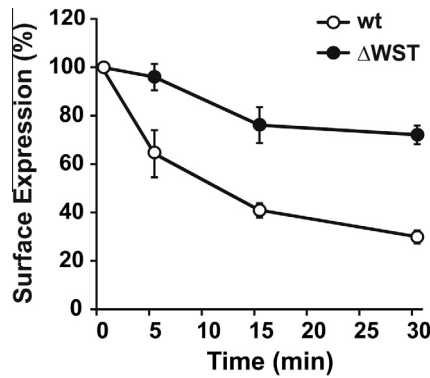


Fig. 5. Internalization of cell surface NHE6 wild-type and Δ WST mutant proteins in AP-1 cells. Kinetics of endocytosis measured in AP-1 cells transiently expressing ^3F NHE6_{HA} wild-type or Δ WST mutant using a cell-based enzyme-linked immunosorbent assay (ELISA). Forty-eight hours post-transfection, surface NHE6 was labeled on ice using a mouse monoclonal anti-Flag antibody, followed by internalization of the anti-Flag-labeled NHE6 at 37 °C for the indicated time points. Remaining cell surface NHE6 was labeled with a goat anti-mouse HRP-conjugated secondary antibody and detected using the fluorescent Amplex[®] Red substrate. Data points represent mean \pm S.E.M. of three different experiments, each done in triplicate.

intensity of internalized Tfn–Alexa⁶³³ was measured in 10^4 live (i.e., 7-AAD negative) GFP-positive HeLa cells. As illustrated in Fig. 7A, cells expressing NHE6wt_{GFP} exhibited a statistically significant increase in transferrin uptake (\sim 35%) compared to GFP-only expressing cells. However, this stimulation was absent in cells expressing NHE6 Δ WST_{GFP}, suggesting that the mutant is deficient in regulating the uptake of transferrin and possibly other cargo internalized via AP2/clathrin-dependent endocytosis. To validate that the measured fluorescent signal was due to receptor-mediated uptake of

transferrin rather than non-specific bulk endocytosis, parallel competition experiments were performed in the presence of excess unlabelled transferrin. As shown in Fig. 7B, the fluorescent signal was dramatically reduced to background levels in the presence of 10-fold competing unlabelled transferrin, suggesting that our measurements are due to specific receptor-mediated endocytosis of fluorescently-labeled transferrin.

3.6. The distribution of the NHE6 Δ WST mutant is altered in primary mouse hippocampal neurons

The above data show that NHE6 Δ WST is mislocalized in non-neuronal and neuroblastoma cell lines. To investigate whether the subcellular distribution of the mutant protein is altered in primary neurons similar to that observed in established cell lines, primary cultures of differentiated mouse hippocampal pyramidal neurons (10–12 days in culture) were transfected with fluorescent mCherry (ChFP) alone or ChFP-tagged constructs of NHE6wt and NHE6 Δ WST and visualized by confocal microscopy after 48 h. As expected, expression of ChFP alone (Fig. 8A and B) was found uniformly throughout the transfected neurons. Conversely, NHE6wt_{ChFP} (Fig. 8D and E) was detected in punctate structures both in the soma and along the neurite projections of transfected neurons in a pattern that mirrored the endogenous protein (Deane et al., 2013). By contrast, NHE6 Δ WST_{ChFP} showed a very diffuse distribution (Fig. 8G and H). Strikingly, while both ChFP- and NHE6wt_{ChFP}-transfected neurons possessed between three to seven first-order neurites as well as secondary and higher-order extensions (\sim 10 transfected cells were examined per construct), neurons expressing NHE6 Δ WST_{ChFP} had a retracted appearance with very few processes, displaying a maximum of three to four first-order branches, but no higher-order branches were evident. To better visualize these morphological differences, the fluorescent images were digitally converted to inverted black and white

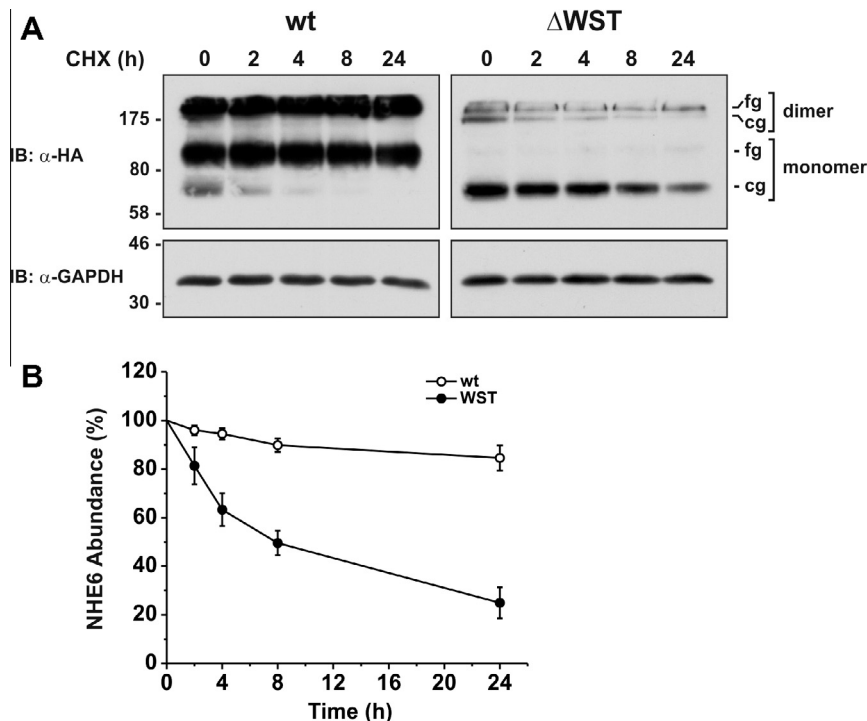


Fig. 6. Stability of NHE6 wild-type and Δ WST mutant proteins in AP-1 cells. (A) AP-1 cells stably expressing ^3F NHE6_{HA} wild-type or Δ WST mutant were treated with 150 $\mu\text{g}/\text{mL}$ cycloheximide for the indicated time points, lysed and analyzed by immunoblotting with a mouse monoclonal anti-HA antibody. Equal amounts of proteins were loaded, as shown by immunoblotting of the same membranes with an anti-GAPDH antibody. (B) Densitometry analysis of ^3F NHE6_{HA} wild-type and Δ WST protein abundance as a function of time in the presence of cycloheximide. Error bars represent the mean \pm S.E.M. of four separate experiments.

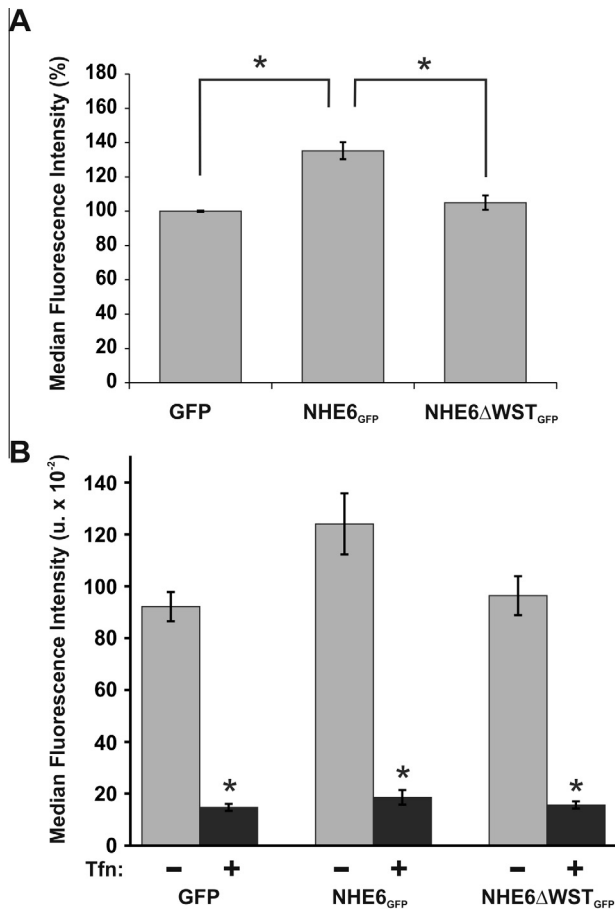


Fig. 7. Regulation of transferrin uptake in HeLa cells expressing NHE6 wild-type and ΔWST. (A) Uptake of Tfn–Alexa⁶³³ (10 μg/mL, 5 min) was monitored in viable HeLa cells expressing GFP alone, NHE6_{GFP} or NHE6ΔWST_{GFP}. (B) Uptake of Tfn–Alexa⁶³³ (10 μg/mL, 5 min) in HeLa cells expressing GFP, NHE6_{GFP} or NHE6ΔWST_{GFP} in the absence (–) or presence (+) of 10-fold excess unlabelled transferrin (Tfn). Median fluorescence intensity of Tfn–Alexa⁶³³ was measured in 10,000 GFP-positive and live cells (*i.e.*, 7-AAD negative) by flow cytometry. Data represent the mean ± S.E.M. of three different experiments. Statistical significance ($p < 0.05$) was evaluated using a paired two-tailed Student's *t*-test and indicated by an asterisk.

images with background or non-specific signals subtracted (Fig 8C, F and I for ChFP, NHE6wt_{ChFP} and NHE6ΔWST_{ChFP}, respectively). While the basis for these profound cellular changes remains to be investigated more thoroughly, these initial observations suggest that expression of the deletion mutant, even in the presence of endogenous NHE6, might impair the normal maintenance of neurite projections.

4. Discussion

Recent studies have identified several mutations in human NHE6/SLC9A6 associated with profound neurodevelopmental and cognitive impairments that present as three broadly overlapping clusters of clinical features. They range from those typical of Christianson syndrome (*i.e.*, mental retardation, mutism, minor craniofacial dysmorphism, epilepsy, ophthalmoplegia, truncal ataxia, emaciation, microcephaly, cerebellar and brainstem atrophy) (Christianson et al., 1999; Riess et al., 2013; Mignot et al., 2013) to those that include additional behaviors characteristic of Angelman syndrome such as frequent laughter/smiling, flexed arms and hyperkinetic movements (Gilfillan et al., 2008; Schroer et al., 2010; Takahashi et al., 2011) and lastly to a novel phenotype

described by Garbern et al. (2010) that shares many of the aforementioned traits but the patients exhibit only occasional mild microcephaly (two out of five patients), modest gross motor disability and absence of the dysmorphic features attributed to the Christianson and Angelman-like syndromes. In addition, the latter phenotype was distinguished clinically by the high prevalence of autistic behavior and biochemically by neuronal and glial inclusions of the microtubule-binding protein tau in cortical and sub-cortical regions that are characteristic of adult-onset neurodegenerative disorders such as Alzheimer's disease. However, it remains unclear how defects in NHE6 cause this spectrum of neurodegeneration in humans. Most of these mutations are nonsense or frameshift alterations that introduce a premature stop codon in the N-terminal catalytic domain of the exchanger, resulting in a severely truncated protein that is unlikely to be functional.

Here, we examined a unique mutation reported by Garbern et al. (2010) that results in the in-frame deletion of three amino acids (³⁷⁰Trp–Ser–Thr³⁷², ΔWST) adjoining the predicted ninth transmembrane segment of NHE6. This tripeptide sequence is relatively conserved in organellar-type NHEs (*i.e.*, NHE6, 7 and 9) compared to plasma membrane-type NHEs (*i.e.*, NHE1–5). The precise evolutionary or structure–function significance of this conservation is unknown, but as discussed below may be important for efficient protein folding of this subgroup of NHEs which share only 39% amino acid identity with their plasma membrane paralogs (Orlowski and Grinstein, 2011). We found that this mutation causes the expressed protein to be largely retained in the ER, although small amounts were partially or fully processed post-translationally and sorted to the plasma membrane in established fibroblastic and neuroblastoma cell lines. A similar pattern of expression was also observed in transfected primary hippocampal neurons. However, endocytosis into recycling endosomes and the overall half-life of the mutant protein were significantly reduced in comparison to wild-type. Indeed, unlike wild-type NHE6, very little if any NHE6ΔWST was detectable in recycling endosomes. This would also be consistent with our observation that the mutant exchanger lost the ability to regulate the trafficking of other recycling endosomal cargo such as the ligand-activated transferrin receptor into NHE6-containing endosomes. This finding corroborates recent studies by Xinhan et al. (2011) demonstrating that overexpression or knockdown of NHE6 in HeLa cells selectively up- or down-regulates, respectively, the internalization of ligand-activated transferrin receptors which is dependent on the endocytic adaptor protein AP2 and clathrin. Notably, this effect was reliant on the ability of NHE6 to regulate intravesicular pH (Xinhan et al., 2011). Indeed, optimal control of organellar pH has long been recognized as an important determinant of vesicular biogenesis, trafficking and/or function (Mellman, 1992; Weisz, 2003). However, no discernible effects were observed for internalization of other cargo such as cholera toxin B and the ligand-activated EGF receptor which are sorted by different, albeit overlapping, pathways (Montesano et al., 1982; Kazacic et al., 2009), suggesting that NHE6 is involved in the regulation of a sub-population of endosomes. Intriguingly, in a separate study in hepatoma HepG2 cells (Ohgaki et al., 2010), knockdown of NHE6 expression resulted in the gradual loss of bulk membrane lipids and bile canalicular proteins from the apical surface, thereby implicating a role for NHE6 and the apical endosomal recycling system in maintenance of cell polarity. At present, the catalytic status of the NHE6ΔWST mutant and its potential effects on pH homeostasis of the ER, if any, are unknown and a subject of ongoing investigation.

The involvement of the recycling endosomal system in neuronal growth, synaptogenesis and plasticity is a subject of intense investigation. In rodent brain, discrete endosomal compartments have been identified at dendritic spines (Cooney et al., 2002; Blanpied et al., 2002; Park et al., 2004, 2006; Racz et al., 2004; Petri

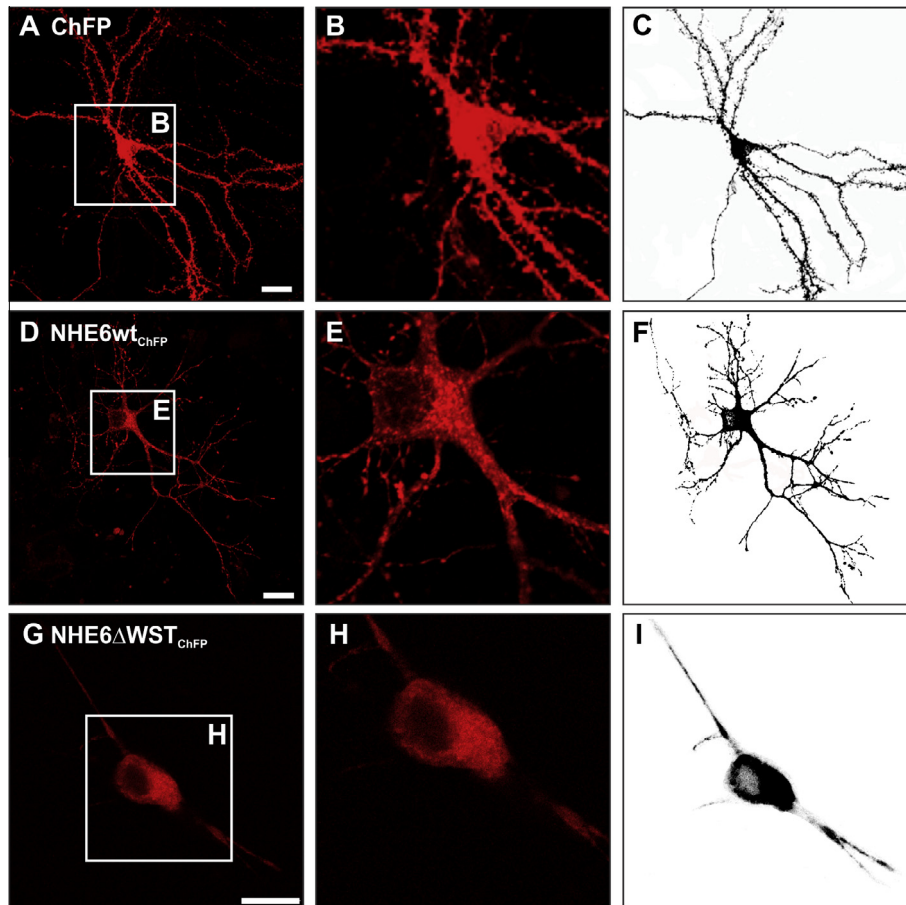


Fig. 8. Subcellular distribution of mCherry-tagged (ChFP) NHE6 wild-type and Δ WST mutant proteins in mouse primary hippocampal neurons. Primary cultures of mouse hippocampal neurons (10–12 days in culture) were transfected with ChFP alone (A–C) NHE6wt_{ChFP} (D–F) or NHE6 Δ WST_{ChFP} (G–I) using a calcium phosphate-DNA coprecipitation method. Following 48 h post-transfection, the cells were fixed in 4% paraformaldehyde/PBS for 20 min at room temperature and mounted onto glass coverslips. Cells were examined by laser scanning confocal microscopy. Scale bars represent 20 μ m.

et al., 2009; Kennedy et al., 2010) and interventions that acutely disrupt vesicular trafficking in hippocampal neurons cause a rapid decline in dendritic spine size and density and also block long-term potentiation (Park et al., 2006). We have recently shown that NHE6 is also a component of recycling endosomes located primarily at the base and head of dendritic spines as well as at presynaptic terminals of cultured mouse hippocampal neurons (Deane et al., 2013). In dendrites and dendritic spines, NHE6 exhibited a high degree of colocalization with vesicles containing the AMPA receptor subunit GluA1. Notably, these vesicles were rapidly mobilized to spine heads following NMDA receptor-dependent stimulation of neuronal activity, thereby implicating a role for NHE6-containing vesicles in synapse formation, maturation, and plasticity.

The importance of NHE6 in endosomal biogenesis and trafficking in the CNS is further highlighted by recent studies of *Nhe6*^{−/−} mice. Disruption of NHE6 function by transgenic insertion of a LacZ reporter gene into the *Nhe6* genomic locus causes a neurodegenerative phenotype that is similar, albeit less pronounced, than that observed in humans (Stromme et al., 2011). The knockout mice exhibit mild motor hyperactivity and cerebellar dysfunction that correlate histologically with disruption of cargo processing along the endosomal-lysosomal pathway of neurons in select regions of the CNS, particularly the basolateral nuclei of the amygdala, the CA3 and CA4 regions and dentate gyrus of the hippocampus and some areas of cerebral cortex. Neuroaxonal dystrophy was also observed in the cerebellum and was accompanied by a marked and progressive loss of Purkinje cells which partially mimics the pathological

and clinical disease features observed in humans with mutations in NHE6.

The precise molecular mechanism by which the Δ WST mutation of NHE6 leads to a severe neurodegenerative phenotype in humans still remains obscure. However, based on the results presented herein and the aforementioned published observations, the accumulation of the NHE6 Δ WST in the ER might generate a pathological state termed ER stress. This would trigger a complex homeostatic mechanism called the unfolded protein response (UPR), which includes a shutdown of global new protein synthesis accompanied by an upregulation of genes important for protein folding (like chaperones) or degradation of misfolded proteins, as well as increased protein export to the cytosol for ubiquitination and proteasome-mediated degradation (Marciniak and Ron, 2006; Doyle et al., 2011; Viana et al., 2012). However, like many neurodegenerative diseases which arise from impaired protein folding (including Alzheimer disease, Parkinson's disease and Huntington's disease), the UPR is not always sufficient to rescue the cell and apoptosis will follow. This occurs especially in post-mitotic neurons, which are not protected from the accumulation of misfolded proteins through the dilution of the ER following cell division (Roussel et al., 2013), providing a putative explanation for the degeneration of certain neurons observed in the patients with the NHE6 Δ WST mutation reported by Garbern et al. (2010). Moreover, activation of the ER stress response might also explain the accumulation of tau-positive fibrillary tangles implicated in the progressive neurodegeneration of these patients (Garbern

et al., 2010). ER stress is known to activate several kinases, like inositol-requiring kinase 1 (IRE1) which activates apoptosis signal-regulating kinase 1 (ASK1) that, in turn, stimulates c-Jun N-terminal kinase (JNK) (Urano et al., 2000; Tabas and Ron, 2011). JNK has been shown to phosphorylate tau at two residues (Thr205 and Ser422) (Reynolds et al., 1997), triggering tau aggregation and formation of neurofibrillary tangles (Vogel et al., 2009). In addition to JNK, glycogen synthase kinase-3 β (GSK-3 β) is another kinase activated by ER stress which hyper-phosphorylates tau and contributes to the formation of neurofibrillary tangles (Jope and Johnson, 2004; Kim et al., 2005). In addition, the subsequent poor posttranslational processing and sorting of NHE6 Δ WST to the plasma membrane and recycling endosomes could further impair optimal vesicular trafficking of postsynaptic (and possible presynaptic) cargo, such as ion channels, neurotransmitter receptors, scaffolding molecules and signal transduction modulators. Ultimately, such cellular disruptions would have the potential to severely impact neuronal function and could account, at least in part, for our preliminary observation that primary hippocampal neurons expressing NHE6 Δ WST exhibit a dramatic reduction in dendritic branching. However, more extensive experimentation is required to verify the nature of this effect and is currently ongoing.

In conclusion, this study provides the first experimental clues to begin deciphering the molecular mechanisms underlying the severe neurodegenerative phenotype observed in patients carrying the Δ WST deletion mutation in the endosomal alkali cation/proton exchanger NHE6. The processing and maturation of this mutant protein are impaired in established cell lines, leading to its decreased stability, defective trafficking, and compromised function in terms of regulating endocytosis of selective cargo. Furthermore, the trafficking of this mutant NHE6 is severely impaired in mouse hippocampal neurons, where it shows a diffuse distribution and induces an apparent reduction in dendritic arborization.

Acknowledgments

We thank Mica Das Gupta and Cassandra McEwan for technical assistance. We also acknowledge the technical assistance provided by the McGill Life Sciences Imaging Facility and Genome Quebec. This work was supported by Canadian Institutes of Health Research funding held by R.A.M. (MOP-86724) and J.O. (MOP-111191).

References

- Barriere, H., Apaja, P., Okiyoneda, T., Lukacs, G.L., 2011. Endocytic sorting of CFTR variants monitored by single-cell fluorescence ratiometric image analysis (FRIA) in living cells. *Methods Mol. Biol.* 741, 301–317.
- Blanpied, T.A., Scott, D.B., Ehlers, M.D., 2002. Dynamics and regulation of clathrin coats at specialized endocytic zones of dendrites and spines. *Neuron* 36, 435–449.
- Brett, C.L., Wei, Y., Donowitz, M., Rao, R., 2002. Human Na⁺/H⁺ exchanger isoform 6 is found in recycling endosomes of cells, not in mitochondria. *Am. J. Physiol. Cell Physiol.* 282, C1031–C1041.
- Christianson, A.L., Stevenson, R.E., van der Meyden, C.H., Pelser, J., Theron, F.W., van Rensburg, P.L., Chandler, M., Schwartz, C.E., 1999. X linked severe mental retardation, craniofacial dysmorphism, epilepsy, ophthalmoplegia and cerebellar atrophy in a large South African kindred is localised to Xq24-q27. *J. Med. Genet.* 36, 759–766.
- Cooney, J.R., Hurlburt, J.L., Selig, D.K., Harris, K.M., Fiala, J.C., 2002. Endosomal compartments serve multiple hippocampal dendritic spines from a widespread rather than a local store of recycling membrane. *J. Neurosci.* 22, 2215–2224.
- Deane, E.C., Ilie, A.E., Sizdahkhani, S., Das Gupta, M., Orlowski, J., McKinney, R.A., 2013. Enhanced recruitment of endosomal Na⁺/H⁺ exchanger NHE6 into dendritic spines of hippocampal pyramidal neurons during NMDA receptor-dependent long-term potentiation. *J. Neurosci.* 33, 595–610.
- Dorner, A.J., Bole, D.G., Kaufman, R.J., 1987. The relationship of N-linked glycosylation and heavy chain-binding protein association with the secretion of glycoproteins. *J. Cell Biol.* 105, 2665–2674.
- Doyle, K.M., Kennedy, D., Gorman, A.M., Gupta, S., Healy, S.J., Samali, A., 2011. Unfolded proteins and endoplasmic reticulum stress in neurodegenerative disorders. *J. Cell Mol. Med.* 15, 2025–2039.
- Garbern, J.Y., Neumann, M., Trojanowski, J.Q., Lee, V.M., Feldman, G., Norris, J.W., Friez, M.J., Schwartz, C.E., Stevenson, R., Sima, A.A., 2010. A mutation affecting the sodium/proton exchanger, SLC9A6, causes mental retardation with tau deposition. *Brain* 133, 1391–1402.
- Géczi, J., Shoubridge, C., Corbett, M., 2009. The genetic landscape of intellectual disability arising from chromosome X. *Trends Genet.* 25, 308–316.
- Gilfillan, G.D. et al., 2008. SLC9A6 mutations cause X-linked mental retardation, microcephaly, epilepsy and ataxia, a phenotype mimicking Angelman syndrome. *Am. J. Hum. Genet.* 82, 1003–1010.
- Humeau, Y., Gambino, F., Chelly, J., Vitale, N., 2009. X-linked mental retardation: focus on synaptic function and plasticity. *J. Neurochem.* 109, 1–14.
- Inlow, J.K., Restifo, L.L., 2004. Molecular and comparative genetics of mental retardation. *Genetics* 166, 835–881.
- Jiang, M., Chen, G., 2006. High Ca²⁺-phosphate transfection efficiency in low-density neuronal cultures. *Nat. Protoc.* 1, 695–700.
- Jope, R.S., Johnson, G.V., 2004. The glamour and gloom of glycogen synthase kinase-3. *Trends Biochem. Sci.* 29, 95–102.
- Kazacic, M., Bertelsen, V., Pedersen, K.W., Vuong, T.T., Grandal, M.V., Rodland, M.S., Traub, L.M., Stang, E., Madhus, L.H., 2009. Epsin 1 is involved in recruitment of ubiquitinated EGF receptors into clathrin-coated pits. *Traffic* 10, 235–245.
- Kennedy, M.J., Davison, I.G., Robinson, C.G., Ehlers, M.D., 2010. Syntaxin-4 defines a domain for activity-dependent exocytosis in dendritic spines. *Cell* 141, 524–535.
- Kim, A.J., Shi, Y., Austin, R.C., Werstuck, G.H., 2005. Valproate protects cells from ER stress-induced lipid accumulation and apoptosis by inhibiting glycogen synthase kinase-3. *J. Cell Sci.* 118, 89–99.
- Le Bivic, A., Real, F.X., Rodriguez-Boulan, E., 1989. Vectorial targeting of apical and basolateral plasma membrane proteins in a human adenocarcinoma epithelial cell line. *Proc. Natl. Acad. Sci. USA* 86, 9313–9317.
- Lein, E.S., Zhao, X., Gage, F.H., 2004. Defining a molecular atlas of the hippocampus using DNA microarrays and high-throughput in situ hybridization. *J. Neurosci.* 24, 3879–3889.
- Leonard, H., Wen, X., 2002. The epidemiology of mental retardation: challenges and opportunities in the new millennium. *Ment. Retard. Dev. Disabil. Res. Rev.* 8, 117–134.
- Lubs, H.A., Stevenson, R.E., Schwartz, C.E., 2012. Fragile X and X-linked intellectual disability: four decades of discovery. *Am. J. Hum. Genet.* 90, 579–590.
- Marciniak, S.J., Ron, D., 2006. Endoplasmic reticulum stress signaling in disease. *Physiol. Rev.* 86, 1133–1149.
- Mellman, I., 1992. The importance of being acid: the role of acidification in intracellular membrane traffic. *J. Exp. Biol.* 172, 39–45.
- Mignot, C., Heron, D., Bursztyn, J., Momtchilova, M., Mayer, M., Whalen, S., Legall, A., Billete, d.V., Burglen, L., 2013. Novel mutation in SLC9A6 gene in a patient with Christianson syndrome and retinitis pigmentosa. *Brain Dev.* 35, 172–176.
- Mitra, N., Sinha, S., Ramya, T.N., Suroliya, A., 2006. N-linked oligosaccharides as outfitters for glycoprotein folding, form and function. *Trends Biochem. Sci.* 31, 156–163.
- Miyazaki, E., Sakaguchi, M., Wakabayashi, S., Shigekawa, M., Mihara, K., 2001. NHE6 protein possesses a signal peptide destined for endoplasmic reticulum membrane and localizes in secretory organelles of the cell. *J. Biol. Chem.* 276, 49221–49227.
- Montesano, R., Roth, J., Robert, A., Orci, L., 1982. Non-coated membrane invaginations are involved in binding and internalization of cholera and tetanus toxins. *Nature* 296, 651–653.
- Morris, M., Maeda, S., Vossel, K., Mucke, L., 2011. The many faces of tau. *Neuron* 70, 410–426.
- Ohgaki, R., Matsushita, M., Kanazawa, H., Ogihara, S., Hoekstra, D., Van IJzendoorn, S.C., 2010. The Na⁺/H⁺ exchanger NHE6 in the endosomal recycling system is involved in the development of apical bile canalicular surface domains in HepG2 cells. *Mol. Biol. Cell* 21, 1293–1304.
- Orlowski, J., Grinstein, S., 2007. Emerging roles of alkali cation/proton exchangers in organellar homeostasis. *Curr. Opin. Cell Biol.* 19, 483–492.
- Orlowski, J., Grinstein, S., 2011. Na⁺/H⁺ exchangers. *Compr. Physiol.* 1, 2083–2100.
- Park, M., Penick, E.C., Edwards, J.G., Kauer, J.A., Ehlers, M.D., 2004. Recycling endosomes supply AMPA receptors for LTP. *Science* 305, 1972–1975.
- Park, M., Salgado, J.M., Ostroff, L., Helton, T.D., Robinson, C.G., Harris, K.M., Ehlers, M.D., 2006. Plasticity-induced growth of dendritic spines by exocytic trafficking from recycling endosomes. *Neuron* 52, 817–830.
- Petrini, E.M., Lu, J., Cognet, L., Lounis, B., Ehlers, M.D., Choquet, D., 2009. Endocytic trafficking and recycling maintain a pool of mobile surface AMPA receptors required for synaptic potentiation. *Neuron* 63, 92–105.
- Racz, B., Blanpied, T.A., Ehlers, M.D., Weinberg, R.J., 2004. Lateral organization of endocytic machinery in dendritic spines. *Nat. Neurosci.* 7, 917–918.
- Reynolds, C.H., Utton, M.A., Gibb, G.M., Yates, A., Anderton, B.H., 1997. Stress-activated protein kinase/c-jun N-terminal kinase phosphorylates tau protein. *J. Neurochem.* 68, 1736–1744.
- Riess, A., Rossier, E., Kruger, R., Dufke, A., Beck-Weedl, S., Horber, V., Alber, M., Glaser, D., Riess, O., Tzschach, A., 2013. Novel SLC9A6 mutations in two families with Christianson syndrome. *Clin. Genet.* 83, 596–597.
- Ropers, H.H., 2010. Genetics of early onset cognitive impairment. *Annu. Rev. Genomics Hum. Genet.* 11, 161–187.
- Rotin, D., Grinstein, S., 1989. Impaired cell volume regulation in Na⁺-H⁺ exchange-deficient mutants. *Am. J. Physiol.* 257, C1158–C1165.
- Roussel, B.D., Kruppa, A.J., Miranda, E., Crowther, D.C., Lomas, D.A., Marciniak, S.J., 2013. Endoplasmic reticulum dysfunction in neurological disease. *Lancet Neurol.* 12, 105–118.

- Roxrud, I., Raiborg, C., Gilfillan, G.D., Stromme, P., Stenmark, H., 2009. Dual degradation mechanisms ensure disposal of NHE6 mutant protein associated with neurological disease. *Exp. Cell Res.* 315, 3014–3027.
- Ruddock, L.W., Molinari, M., 2006. N-glycan processing in ER quality control. *J. Cell Sci.* 119, 4373–4380.
- Schroer, R.J., Holden, K.R., Tarpey, P.S., Matheus, M.G., Griesemer, D.A., Friez, M.J., Fan, J.Z., Simensen, R.J., Stromme, P., Stevenson, R.E., Stratton, M.R., Schwartz, C.E., 2010. Natural history of Christianson syndrome. *Am. J. Med. Genet. A* 152A, 2775–2783.
- Shi, S., Hayashi, Y., Esteban, J.A., Malinow, R., 2001. Subunit-specific rules governing AMPA receptor trafficking to synapses in hippocampal pyramidal neurons. *Cell* 105, 331–343.
- Stromme, P., Dobrenis, K., Sillitoe, R.V., Gulinello, M., Ali, N.F., Davidson, C., Micsenyi, M.C., Stephney, G., Ellevog, L., Klungland, A., Walkley, S.U., 2011. X-linked Angelman-like syndrome caused by Slc9a6 knockout in mice exhibits evidence of endosomal-lysosomal dysfunction. *Brain* 134, 3369–3383.
- Tabas, I., Ron, D., 2011. Integrating the mechanisms of apoptosis induced by endoplasmic reticulum stress. *Nat. Cell Biol.* 13, 184–190.
- Takahashi, Y., Hosoki, K., Matsushita, M., Funatsuka, M., Saito, K., Kanazawa, H., Goto, Y., Saitoh, S., 2011. A loss-of-function mutation in the SLc9A6 gene causes X-linked mental retardation resembling Angelman syndrome. *Am. J. Med. Genet. B Neuropsychiatr. Genet.* 156B, 799–807.
- Tzschach, A., Ullmann, R., Ahmed, A., Martin, T., Weber, G., Decker-Schwering, O., Pauly, F., Shamdeen, M.G., Reith, W., Oehl-Jaschkowitz, B., 2011. Christianson syndrome in a patient with an interstitial Xq26.3 deletion. *Am. J. Med. Genet. A* 155A, 2771–2774.
- Urano, F., Wang, X., Bertolotti, A., Zhang, Y., Chung, P., Harding, H.P., Ron, D., 2000. Coupling of stress in the ER to activation of JNK protein kinases by transmembrane protein kinase IRE1. *Science* 287, 664–666.
- Vaillend, C., Poirier, R., Laroche, S., 2008. Genes, plasticity and mental retardation. *Behav. Brain Res.* 192, 88–105.
- Viana, R.J., Nunes, A.F., Rodrigues, C.M., 2012. Endoplasmic reticulum enrollment in Alzheimer's disease. *Mol. Neurobiol.* 46, 522–534.
- Vogel, J., Anand, V.S., Ludwig, B., Nawoschik, S., Dunlop, J., Braithwaite, S.P., 2009. The JNK pathway amplifies and drives subcellular changes in tau phosphorylation. *Neuropharmacology* 57, 539–550.
- Weisz, O.A., 2003. Acidification and protein traffic. *Int. Rev. Cytol.* 226, 259–319.
- Xinhan, L., Matsushita, M., Numaza, M., Taguchi, A., Mitsui, K., Kanazawa, H., 2011. Na⁺/H⁺ exchanger isoform 6 (NHE6/SLC9A6) is involved in clathrin-dependent endocytosis of transferrin. *Am. J. Physiol. Cell Physiol.* 301, C1431–C1444.
- Yuste, R., Bonhoeffer, T., 2001. Morphological changes in dendritic spines associated with long-term synaptic plasticity. *Annu. Rev. Neurosci.* 24, 1071–1089.